Article

Electrostatic Similarity Analysis of Human β-Defensin Binding in the Melanocortin System

Matthew A. Nix,[1] Christopher B. Kaelin,[2,3] Rafael Palomino,[1] Jillian L. Miller,[1] Gregory S. Barsh,[2,3,*] and Glenn L. Millhauser[1,*]

[1]Department of Chemistry and Biochemistry, University of California, Santa Cruz, Santa Cruz, California; [2]HudsonAlpha Institute for Biotechnology, Huntsville, Alabama; and [3]Department of Genetics, Stanford University, Stanford, California

SUMMARY The β-defensins are a class of small cationic proteins that serve as components of numerous systems in vertebrate biology, including the immune and melanocortin systems. Human β-defensin 3 (HBD3), which is produced in the skin, has been found to bind to melanocortin receptors 1 and 4 through complementary electrostatics, a unique mechanism of ligand-receptor interaction. This finding indicates that electrostatics alone, and not specific amino acid contact points, could be sufficient for function in this ligand-receptor system, and further suggests that other small peptide ligands could interact with these receptors in a similar fashion. Here, we conducted molecular-similarity analyses and functional studies of additional members of the human β-defensin family, examining their potential as ligands of melanocortin-1 receptor, through selection based on their electrostatic similarity to HBD3. Using Poisson-Boltzmann electrostatic calculations and molecular-similarity analysis, we identified members of the human β-defensin family that are both similar and dissimilar to HBD3 in terms of electrostatic potential. Synthesis and functional testing of a subset of these β-defensins showed that peptides with an HBD3-like electrostatic character bound to melanocortin receptors with high affinity, whereas those that were anticorrelated to HBD3 showed no binding affinity. These findings expand on the central role of electrostatics in the control of this ligand-receptor system and further demonstrate the utility of employing molecular-similarity analysis. Additionally, we identified several new potential ligands of melanocortin-1 receptor, which may have implications for our understanding of the role defensins play in melanocortin physiology.

INTRODUCTION

β-defensins are small cationic, disulfide-rich proteins of the innate and adaptive immune system that are capable of signaling at melanocortin receptors (MCRs) (1-3). In the melanocortin system, a collection of G-protein-coupled receptors (GPCRs) and their ligands act together to regulate diverse physiological phenomena, including pigmentation, adrenal function, and appetite (4). As GPCRs, the MCRs transmit signals by coupling to intracellular G proteins and, as shown recently for MC4R, inward rectifying potassium channels (5). At melanocortin-1 receptor (Mc1r), which is located in the skin, agonist binding stimulates receptor activation and cyclic AMP production, leading to the synthesis of black/brown eumelanin pigment (6,7). Conversely, inverse-agonist binding at Mc1r decreases receptor signaling and cyclic AMP production, leading to the synthesis of red/yellow pheomelanin pigment (8). At melanocortin-4 receptor (Mc4r), which is found in the hypothalamus, receptor activation leads to a decrease in appetite while a reduction in receptor signaling leads to increased appetite. The classic melanocortin hormones for both of these receptors, including the agonist α-melanocyte stimulating hormone (α-MSH) and the inverse agonists Agouti signaling protein (ASIP) and Agouti-related protein (AgRP), all bind through a well-characterized linear motif of positively charged and aromatic residues, HFRW and RFF, respectively (9-12). Previously, we characterized the newest ligand that is capable of modulating melanocortin signaling, canine β-defensin 3 (CBD103), solving a long-standing mystery regarding the dominant inheritance of black coat color in domestic dogs (2). More recently, we performed a structure-function analysis of the human ortholog of CBD103, human β-defensin 3 (HBD3), to determine the physicochemical properties that confer its high-affinity binding to the MCRs (13). Our analysis of HBD3 uncovered a mechanism for receptor binding that operates in a fundamentally different way than all previously characterized melanocortin ligands. Surprisingly, we found that HBD3 does not rely on any comparable positive-aromatic sequence for receptor binding, such as that found in the melanocortins ASIP and AgRP, but instead depends on electrostatic complementarity between the positively charged β-defensin peptide surface and the negatively charged MCR exo-loops.

Historically the discovery of melanocortin ligands and receptors, including HBD3, has been coupled to

Submitted May 13, 2015, and accepted for publication September 3, 2015.

*Correspondence: gbarsh@hudsonalpha.org or glennm@ucsc.edu

Editor: David Cafiso.

0006-3495/15/11/1946/13

http://dx.doi.org/10.1016/j.bpj.2015.09.005

phenotype-driven pigmentation research. This approach utilizes model organisms that possess unique and identifiable coat-color phenotypes, enabling genetic linkage mapping and pedigree analysis to pinpoint the responsible genetic elements. Therefore, the genetic relationships among melanocortin-system member proteins were well understood before their molecular and structural details were elucidated. One alternative protein-structure-based method for finding molecules with a specific function is molecular-similarity analysis, which is based on the fundamental concept that molecules with similar physicochemical properties will exhibit similar behaviors and functions (14). Molecular-similarity tools, which were originally developed in the field of medicinal chemistry for in silico screening of small-molecule drug candidates, have more recently been adapted for use with larger, more complex biomolecules (14). The application of molecular-similarity analysis, coupled with experimental data, can serve as a valuable search tool for discovering new molecules with specific activity and provide deeper insight into the physicochemical requirements that define their function. From this perspective, and because of the unique electrostatic binding mode employed by HBD3 and the MCRs, we postulated that other β-defensin peptides with properties similar to those of HBD3 might also bind to and signal at the MCRs.

In this study, we performed a molecular-similarity analysis of all known human β-defensin sequences, obtained from the UniProt database, and tested a subset of them for their binding properties at the MCRs. Using the Protein Interaction Property Similarity Analysis (PIPSA) computational tool, which combines Poisson-Boltzmann electrostatic calculations with molecular-similarity analysis, we obtained results that allowed us to categorize β-defensins based on their similarity to the electrostatic potential of HBD3 (15,16). We synthesized and tested a subset of these peptides and found that β-defensins with HBD3-like electrostatic potentials bound with high affinity to Mc1r, whereas β-defensins that were highly dissimilar to HBD3 did not display any affinity. As a result, our investigation identified several new (to our knowledge) potential ligands, some with remarkably high affinity, that may have a relevant signaling function in the melanocortin system. Furthermore, our analysis established the utility of in silico electrostatic similarity methods for discriminating binding function at these receptors. Together, our findings demonstrate that electrostatic potential alone is a primary binding determinant in the melanocortin system, which may lead to further insights into the relationship between β-defensins and melanocortin signaling.

MATERIALS AND METHODS

Protein modeling

All protein models used in this study were generated using the program Modeler, version 9.9 (17). Human β-defensin sequences were obtained from the Universal Protein Resource (UniProt) database (18). All sequences with unknown structures (29 of 32) were aligned to the HBD3 sequence utilizing Modeler's *align2d* alignment routine. When alignment was poor due to low sequence similarity between the target defensin and HBD3, the two sequences were manually aligned using the six canonical cysteine residues present in both sequences as a guide. Aligned sequences were truncated to reflect the approximate length of HBD3. When necessary, sequences were truncated 10 amino acids N-terminal of the first cysteine and four amino acids C-terminal to the last cysteine. Using the sequence alignment and one randomly chosen NMR model from the published HBD3 structure (PDB ID: 1kj6) as a structural template, we generated new defensin models using Modeler's *automodel* routine. We aligned all of the generated β-defensin structures to the HBD3 structure using the *Matchmaker* tool in Chimera, and saved their PDB coordinates before using them in molecular-similarity calculations (19). Note that our subsequent calculations did not depend on which low-energy NMR structures we chose from 1kj6.

Electrostatic calculations and similarity analysis

The electrostatic calculations and similarity analysis were performed using the PIPSA software package (15,16). All β-defensin PDB structure files (both homology modeled and obtained from the PDB database) were converted to PQR files using the PDB2PQR program with an AMBER force field. The protonation state of the titratable amino acids was automatically assigned using the program PROKPA (a component of the PDB2PQR program) and was performed at pH 7.0. Electrostatic potentials were calculated using the adaptive Poisson-Boltzmann solver (APBS) and the similarity analysis was performed by PIPSA (20,21). The APBS and environmental parameters included a grid spacing of 1 Å, a simulated temperature of 300 K, and a 50 mM solvent ionic strength. A 50 mM solvent ionic strength was chosen primarily for convenience (the default setting in PIPSA) but also as an intermediate value between a 0 mM strength (which may overemphasize differences electrostatically) and a 150 mM strength (which would decrease the electrostatic difference and compress the similarity comparison). A similarity analysis utilizing variable ionic strength values did not significantly alter the electrostatic ranking. The solvent dielectric constant was set to 78 and the protein interior dielectric constant was 2. The Hodgkin electrostatic similarity index (ESI) and Carbo ESI were calculated and subjected to a complete cluster analysis using the statistical program R (22,23). Although we calculated both the Hodgkin and Carbo indices, in this study we report only the Hodgkin indices. This is primarily because Hodgkin indices (according to the form of the equation) are more sensitive to differences in both the magnitude and form of the electrostatic potential, whereas Carbo indices are sensitive to form but not magnitude.

Peptide synthesis

All peptides were produced on a CEM Liberty1 microwave peptide synthesizer using standard Fmoc chemistry. Amino acids were purchased from Aapptec and assembled on H-Rink amide ChemMatrix resin purchased from Aldrich. Fmoc protecting groups were removed using 20% piperidine with 0.1 M hydroxybenzotriazole in dimethylformamide. Amino acids were coupled using 5 molar equivalents of diisopropylcarbodiimide and 10 molar equivalents of hydroxybenzotriazole in dimethylformamide. N-terminal capping was achieved when necessary with a 10% solution of acetic anhydride. Cleavage of the peptide from the resin was performed in a mixture of TFA/TIS/EDT/phenol (90:4:4:2) for 90 min. Crude products were purified by preparative reverse-phase high-performance liquid chromatography (RP-HPLC) and identified by electrospray ionization mass spectrometry before they were subjected to oxidative folding reactions. Quantitative concentrations were determined via amino

acid analysis at the Molecular Structure Facility, University of California, Davis.

Oxidative peptide folding and characterization

To produce folded peptides with the native β-defensin disulfide bond connectivity of Cys-1-5, Cys-2-4, and Cys-3-6, all peptides were folded using either a full-orthogonal or semiorthogonal cysteine protection scheme. For peptides produced with full-orthogonal cysteine protection, including HBD3, HBD2, defb29, and defb28, disulfides were formed according to previously published protocols (24). Briefly, peptides were synthesized using three different cysteine precursors with orthogonal side-chain protecting groups. Cys-1 and Cys-5 were protected with the standard Trityl protecting group, which is removed during the initial TFA cleavage step that removes the peptide from the resin. Cys-2 and Cys-4 were protected using the acetamidomethyl (Acm) protecting group, and Cys-3 and Cys-6 were protected with the *tert*-butyl protecting group. The first disulfide (Cys-1-5) was formed using an oxidative folding solution consisting of 50% acetonitrile and 50% water, set to pH 8.0 with ammonium hydroxide. The peptide concentration was typically 0.5 mg/mL. The reaction mixture was stirred overnight at room temperature, followed by lyophilization. The resulting product showed a mass loss of 2 amu as well as resistance to the sulfhydryl alkylating agent *N*-ethylmaleimide (NEM), consistent with the formation of a single disulfide bond. The second disulfide (Cys-2-4) was formed by dissolving the lyophilized product in a 4:1 ratio of glacial acetic acid and 0.1 M HCl to a final concentration of 0.5 mg/mL, followed by the addition of 20 molar equivalents of iodine in glacial acetic acid, which simultaneously removes the Acm protecting group and oxidizes the disulfide (25). The reaction mixture was stirred for 90 min and then quenched by the addition of excess ascorbic acid, and purified by RP-HPLC. The resulting single product showed a mass loss of 144 amu and resistance to NEM modification, consistent with the removal of two Acm protecting groups and the formation of the second disulfide bond. The third and final disulfide (Cys-3-6) was formed by dissolving the peptide to a final concentration of 2 mg/mL in neat TFA with 40 molar equivalents of anisole and 100–300 molar equivalents of either DMSO or diphenyl sulfoxide, which simultaneously removes the *tert*-butyl protecting group and oxidizes the disulfide. When we used diphenyl sulfoxide, we additionally added 150 equivalents of methyltrichlorosilane to catalyze the reaction (26). The reaction mixture was stirred for 1–2 h at room temperature and quenched by adding excess ice-cold ether to precipitate the peptide. The precipitate was redissolved and purified by RP-HPLC, and the resulting single product showed a mass loss of 114 amu, consistent with the removal of the *tert*-butyl protecting groups and formation of the final disulfide bond. For peptides containing a tryptophan residue, including defb25, defb23, defb18, and defb4, we resorted to a semiorthogonal protection scheme due to these residues' susceptibility to modification during the removal of the *tert*-butyl protecting groups. Under this methodology, Cys-2, -3, -4, and -6 were protected using the Trt protecting group, and Cys-1 and -5 were protected with the Acm protecting group. With this method, the number of disulfide bond combinations was reduced from 15 to three, with one of the three representing the native connectivity. The first two disulfide bonds were formed using our standard folding buffer of 10% DMSO, 1.6 M guanidine HCl, and 0.1 M Tris at pH 8.5. Purification by RP-HPLC typically resulted in two or three separable peaks with identical oxidized mass, indicating the presence of most or all combinations of the four free thiols oxidized into two disulfide bonds. To determine which species had the native connectivity of Cys-2-4 and Cys-3-6, we subjected each isolated peak to partial reduction, NEM modification, protease digestion, and fragment identification by matrix-assisted laser desorption/ionization time-of-flight (MALDI-TOF) mass spectrometry. Briefly, ~50 μg of peptide was subjected to partial reducing conditions in 100 mM Tris buffer, pH 5.0, with 1 molar equivalent of the mild reducing agent tris(2-carboxyethyl)phosphine hydrochloride for 15 min at room temperature. A large excess of NEM was then added to the mixture and allowed to incubate for another 15 min before purification by RP-HPLC. The product corresponding to a single disulfide reduction and modification, as identified by a mass increase of 125 amu per thiol, was isolated and lyophilized. The sample was then fully reduced with 20 mM dithiothreitol for 1 h at 37°C and incubated with one of several proteases (Arg-C, Lys-C, trypsin, and chymotrypsin, all provided by Princeton Separations, Freehold Township, NJ) overnight at room temperature to allow for full digestion of the peptide before mass spectrometry analysis (Ettan MALDI-TOF Pro; Amersham Biosciences). Peptide digests and standard mass controls (angiotensin III and adrenocorticotropic hormone) were mixed in a 1:1 ratio with a saturated solution of α-cyano-4-hydroxycinnamic acid matrix compound on MALDI plates. MALDI-TOF analysis was accomplished using a 20 kV acceleration potential in positive ion mode, with both reflectron and linear scanning modes. Digest fragments were predicted by the autodigest simulation tool in Mass Lynx (Waters), accounting for both NEM and Acm cysteine modifications. Since the Acm-protected cysteines did not participate in the initial oxidative fold, we determined the connectivities by identifying matching free thiol or NEM digest fragments. After identifying the species that possessed native β-defensin disulfide connectivity, we formed the final disulfide between Cys-1 and Cys-5 using the previously mentioned reaction with iodine in glacial acetic acid. All folded peptides were purified by RP-HPLC and identified as fully oxidized peptides by mass spectrometry.

Competitive binding assays

Receptor-ligand binding assays were performed using the DELPHIA lanthanide-based detection system on intact human embryonic kidney (HEK) 293T cells transiently transfected with MCR expression constructs as previously described (2).

RESULTS

β-defensin structural modeling

A prerequisite for performing a molecular-similarity analysis is to obtain 3D coordinates of the proteins of interest by either direct structure determination or homology modeling. In the human β-defensin protein family, only four of the 32 known members (HBD1, HBD2, HBD3, and HBD6) have solved structures (27-30). Therefore, we performed homology modeling on all β-defensins of unknown structure using the Modeler program, utilizing HBD3 as a structural template. One difficulty we anticipated was the lack of primary sequence similarity within the β-defensin family, which is a requirement for sequence alignment between the protein to be modeled and the structural template. However, the β-defensins are classified together primarily because of their highly conserved cysteine spacing and disulfide topology, which gives rise to their characteristic fold. The profound influence of the disulfides is seen in three of the β-defensins of known structure insofar as they share little primary sequence similarity, yet remarkably adopt nearly identical folds (Fig. 1) (31). Therefore, the alignment of the cysteines appeared to be the most critical aspect for generating accurate homology models of each defensin. In light of this, we inspected each alignment result to confirm that all cysteine residues of the target and template sequence were aligned properly before proceeding with the modeling calculations. When the cysteines did not align, we

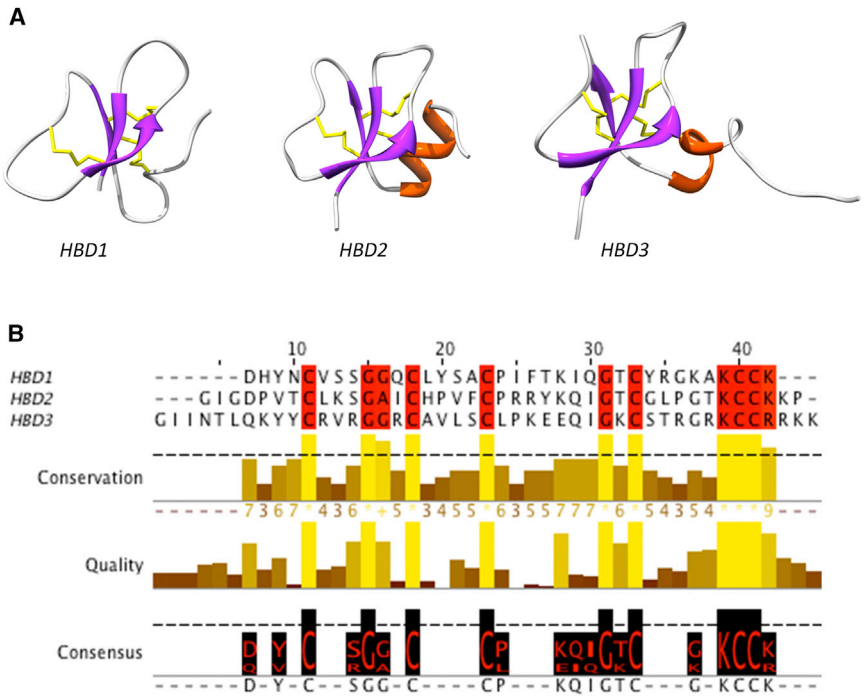

FIGURE 1 β-defensin structures and sequences. (*A*) Structures of HBD1 (PDB ID: 1KJ5), HBD2 (PDB ID: 1FD3), and HBD3 (PDB ID: 1KJ6), shown from left to right. Purple, β-strands; red, α-helices; yellow, disulfide bonds. (*B*) Multiple sequence alignment of the same three β-defensins, highlighting the conserved residues in red.

manually altered the alignment to match them exactly so as to produce structural models that were restrained by these conserved disulfide bonds.

Another consideration for our modeling analyses was that β-defensin sequences vary in length from 36 to more than 100 residues, with extended polypeptide segments outside of the cysteine-rich core (Fig. S1 in the Supporting Material). Consequently, when we initially generated models of the longer sequences, they maintained the typical β-defensin fold induced by the cysteine alignment, but usually had long tails of unknown structure on the N-terminus, C-terminus, or both. We therefore utilized N- or C-terminal truncated versions of these longer β-defensins for modeling and molecular-similarity analysis, as well as for functional testing. We employed this strategy for two reasons. First, to test our electrostatic binding model, we hypothesized that only the folded core component of each β-defensin was necessary. In our previous analysis of HBD3, nearly all of the charged residues required for high-affinity receptor binding were contained in the folded core region, bracketed by the terminal cysteines, and imposed by the disulfide bonds (2). Second, the majority of the amino acid sequences we obtained from the UniProt database are inferred from evidence at the transcription level, which may not accurately reflect the sequence of the final mature form of the protein (32). All three of the β-defensins detected at the protein level have very short N- and C-terminal sequence lengths beyond their six-cysteine core, suggesting that this folded segment alone is sufficient for function. We therefore truncated the longer β-defensin sequences using the native length of HBD3 as our guide. With HBD3, the N-terminus originates 10 residues before the first cysteine, and the C-terminus extends four amino acids beyond the last of the six canonical cysteines (Fig. 1 *B*). To retain a similarly sized folded core for the new β-defensins, we truncated the N- and C-termini of each peptide sequence in a fashion identical to that employed for HBD3 when it was necessary to do so. Fig. 2 shows the truncated β-defensin sequences that were used in this study. After generating 3D models for the set of β-defensins, we visually inspected each result to ensure a reasonably folded structure for the new defensin. We also aligned each model to the PDB coordinates of HBD3 using the Chimera molecular viewing program and its *Matchmaker* function, which is a necessary step to accurately perform similarity analyses.

PIPSA molecular-similarity analysis

The use of molecular-similarity analysis to classify molecules with a particular chemical behavior is a common practice in small-molecule medicinal chemistry (33). More recently, molecular-similarity analysis has been adapted for use with larger, more complex biomolecules such as DNA and proteins. This method aims to use computer-aided comparisons of molecular properties to predict the biological activity of uncharacterized molecules. In general, the application of molecular-similarity methods requires the investigator to make several key choices. First, one must choose an appropriate molecular descriptor that accurately captures the relevant physicochemical qualities of the molecules in question. Molecular descriptors in medicinal chemistry applications can range widely from simple

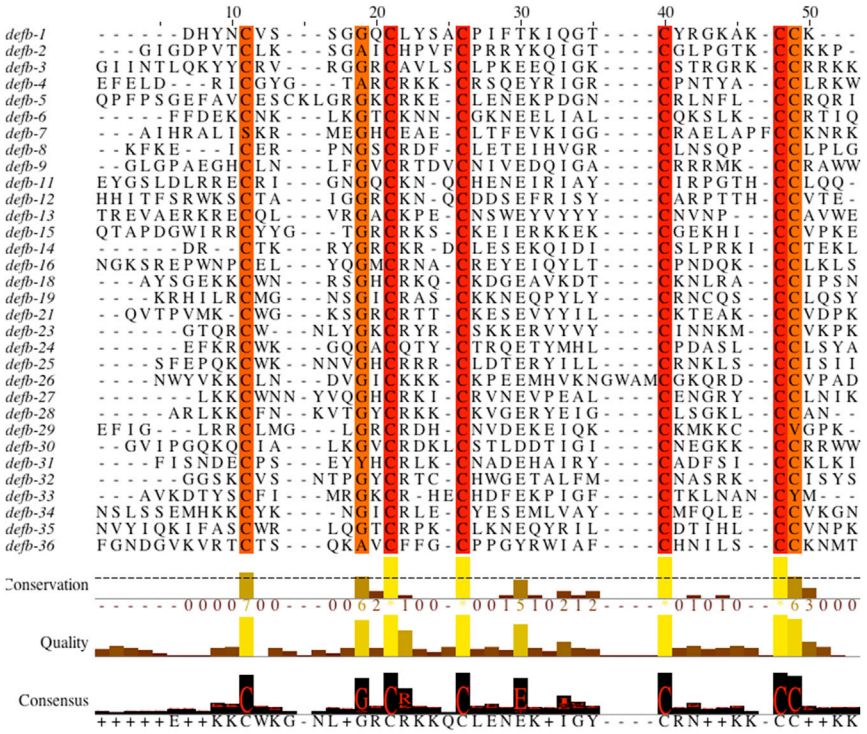

FIGURE 2 Multiple sequence alignment of all truncated human β-defensins employed in this study. When it was necessary, the N-terminus of each new defensin was truncated 10 amino acids before the first cysteine residue, and the C-terminus was truncated four amino acids after the last cysteine, which is similar to the length of mature HBD3.

macroscopic properties such as molecular weight (and others similar to Lipinski's rule of five) to calculated 3D surface properties such as electrostatic potential or hydrophobicity (34-36). The descriptor employed is usually chosen based on prior knowledge of important molecular characteristics of the system being studied. Second, one must choose a method for comparing molecular descriptors, called similarity metrics (37,38). This typically involves mathematical comparisons of the molecular descriptors of two molecules. The output of a similarity metric operation between a descriptor of two molecules is a single numerical value that captures the extent of similarity between them. Finally, in addition to descriptors and metrics, one must choose a mechanism to select molecules that are predicted to exhibit a given chemical behavior. This requires prior knowledge regarding the mechanism of interest in a given system, such as a typical binding mode of a known molecule (an important characteristic that gives a molecule function), or details about the chemical nature of a ligand-binding or enzymatic site.

Our previous structure-function analysis of HBD3 (13) suggested that charge complementarity is the main driving force behind its binding affinity for the MCRs. Therefore, the electrostatic potential of the β-defensins served as our molecular descriptor, with the additional hypothesis that similarity to HBD3 would confer high-affinity binding to the MCRs. The current method for estimating the electrostatic characteristics of proteins involves solving the linearized Poisson-Boltzmann (LPB) equation of a 3D model of the biomolecule (39-42). APBS is a stand-alone software application that is capable of solving the LPB equation for any biomolecule, but it can also be incorporated into other molecular viewing programs as a plug-in (Pymol) or in the computational stream of larger software applications (20).

We chose to use the PIPSA computational tool to perform all aspects of our molecular-similarity analysis. This program incorporates the APBS program to solve the LPB equation, as well as other software components to perform molecular-similarity and cluster analyses of the electrostatic results. We proceeded to perform our molecular-similarity analysis on all 32 human β-defensins using the three known structures (HBD1–3) and our Modeler-generated models.

Fig. 3 displays the results of our PIPSA cluster analysis as a dendrogram, with β-defensin groupings exhibiting a range of electrostatic similarities to HBD3 and to each other. In general, the analysis identified two distinct, high-level clusters, and each cluster was further subdivided to form a total of four major clusters, with the first containing HBD3 (cluster 1). Unsurprisingly, the majority of β-defensins that clustered together with HBD3 (net charge +11) possessed some of the highest net-positive charges in the entire family. We also found several β-defensins that were very dissimilar to those found in cluster 1, some of which were electrostatically anticorrelated to HBD3 according to their ESI scores (cluster 4). Interestingly, several of the peptides in clusters 3 and 4 had net charges similar to those of the β-defensins found in clusters 1 and 2, emphasizing the importance of the arrangement of charged

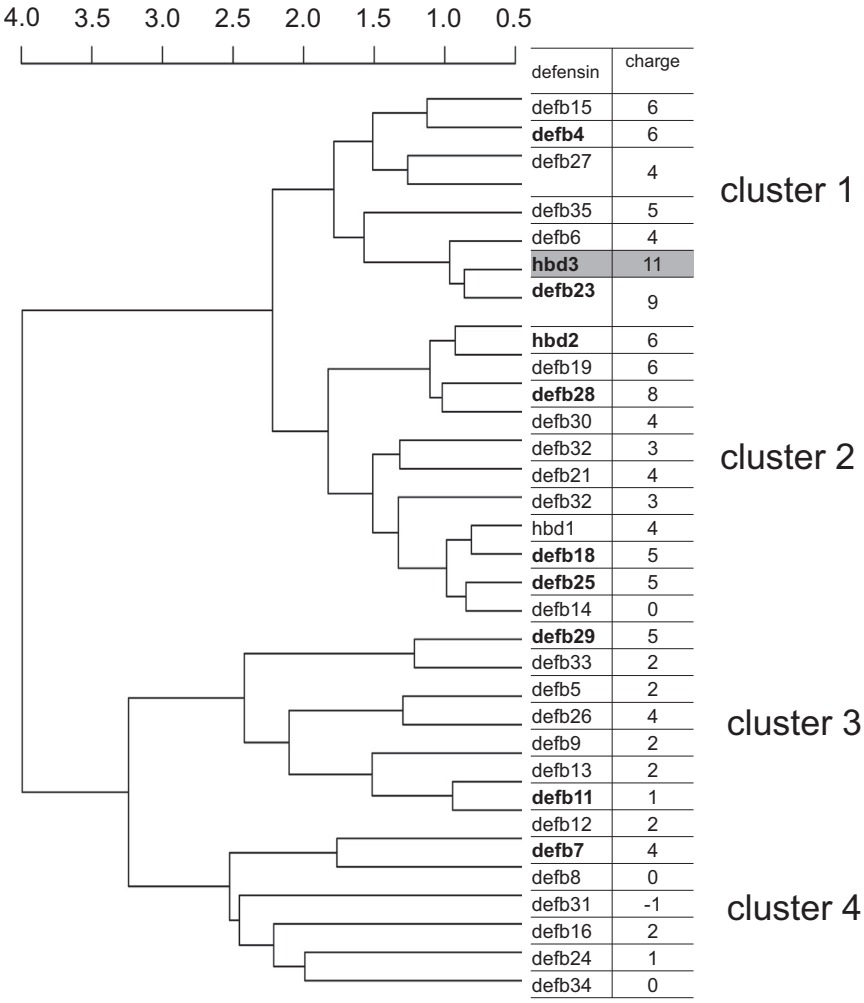

FIGURE 3 PIPSA ESIs displayed as a dendrogram. The electrostatic potentials of all 32 truncated human β-defensins were compared with each other using Hodgkin ESIs. Each peptide's net charge is shown next to its identifier. The location of HBD3 in the cluster analysis is highlighted in gray. The peptides grouped into four distinct clusters, as marked above, according to complete cluster analysis using the R program. Peptides selected for synthesis and functional testing are highlighted in bold.

residues in forming the electrostatic potential field of a protein and not simply the total charge.

Although the dendrogram method of analysis provides unbiased insight into the electrostatic relatedness of a group as a whole, we were primarily interested in determining each peptide's specific electrostatic similarity to HBD3. Fig. 4 displays the raw Hodgkin ESI scores for all β-defensins relative only to HBD3, ranging from 1 (complete similarity) to −1 (complete dissimilarity). According to this method of parsing the data, several peptides that were located in clusters other than cluster 1 (HBD3's cluster) are now shown to have electrostatics highly similar to those of HBD3. We selected several peptides from our analysis for synthesis and functional testing, including defb4, defb23, and hbd2 from cluster 1; defb28, defb18, defb25, and defb29 from cluster 2; defb11 from cluster 3; and defb7 from cluster 4 (Figs. 3 and 4). We selected defb7 because it lacks the first Cys residue and therefore serves as a test of the influence of disulfide cross-links. To establish positive controls for our binding assay, we synthesized and tested HBD3 as well as ASIP-YY, a modified synthetic variant of ASIP that possesses improved folding characteristics (43). Both HBD3 and ASIP-YY have well-established binding constants at Mc1r and Mc4r, falling in the nanomolar range (2). This provided us with a direct comparison to judge the binding affinity of new β-defensins relative to peptides with known affinities.

β-defensin folding

All β-defensin peptides were initially synthesized with free thiols, enabling the use of conventional oxidative folding techniques. After oxidation occurred, however, most of the peptides gave multiple species according to HPLC, suggesting a mixture of native and nonnative disulfide bond arrangements. We considered using disulfide mapping to identify the correctly folded species, but thought that would be exceptionally challenging given the specific defensin sequence and large number of observed conformers. We

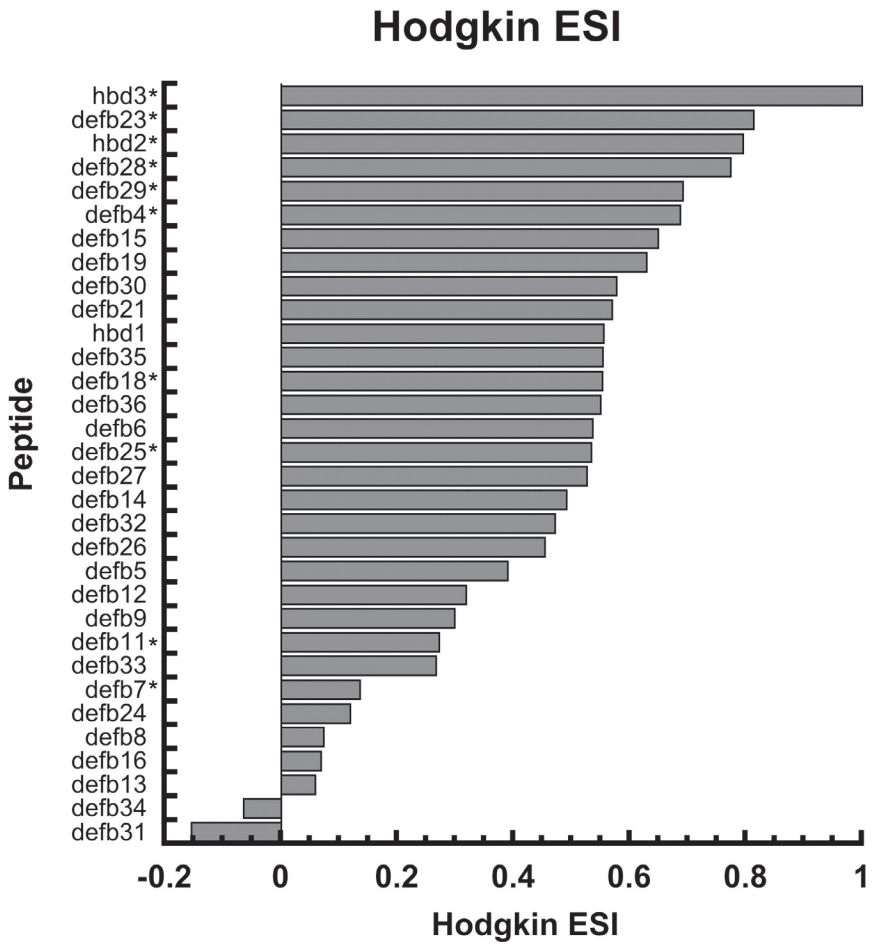

FIGURE 4 PIPSA Hodgkin ESIs for all β-defensins relative to HBD3, ranging from +1 (complete similarity) to −1 (completely dissimilar). HBD3 has an ESI of 1 (complete identity relative to itself). The graph is sorted from highest HBD3 similarity (*top*) to lowest HBD3 similarity (*bottom*). The peptides chosen for synthesis and functional testing are marked with an asterisk (*).

therefore decided to synthesize all β-defensin peptides with orthogonal cysteine-protecting groups, which would allow us to selectively form the native β-defensin disulfide connectivities of Cys-1-5, Cys-2-4, and Cys-3-6. When a peptide sequence was incompatible with the reaction conditions for removing the full-orthogonal cysteine protection groups, we employed a semiorthogonal protection strategy coupled with enzymatic digestion and mass spectrometry to determine the disulfide connectivity (see Materials and Methods). We were able to engineer or determine the native disulfide connectivity for all peptides chosen for synthesis, with the exception of defb4 and defb7. Although our initial synthesis and folding of the free-thiol version of defb4 resulted in a single folded species of unknown disulfide connectivity, we were unable to produce the full or semiorthogonal version necessary to ensure native connectivity. Nevertheless, we included the defb4 peptide in this study with the caveat that its binding results may be inaccurate due to alternative folded states (though we note anecdotally that when multiple conformers were tested in previous studies, they typically exhibited similar binding affinities). In the case of defb7, the native sequence contains only five of the six canonical cysteine residues (missing Cys-1). To simplify the synthesis of this peptide, we replaced Cys-5 with alanine, eliminating disulfide 1-5 altogether. The two remaining native disulfide bonds were formed using orthogonal protecting groups. Although the defb7 binding results are included in this study, they must be considered in the context of less structural rigidity than is assumed in the modeled structure and electrostatic calculations.

β-defensin pharmacology

Fig. 5 shows the results of binding assays for the ligands that exhibited measurable affinity. The primary results of our studies are summarized in Table 1. Of the seven β-defensins selected from clusters 1 and 2, five bound to Mc1r with affinities ranging from strong to moderate, with most K_i values < 200 nM. Two exceptions were defb4 (cluster 1) and defb18 (cluster 2). Defb4 had K_i values in the micromolar range, much weaker than all others in cluster 1. However, as noted above, the disulfide connectivity of this peptide was uncertain, and its weaker binding may be due to improper folding. Unlike other peptides from cluster 2, defb18 exhibited no binding to Mc1r whatsoever. In contrast to peptides from clusters 1 and 2, peptides from clusters 3

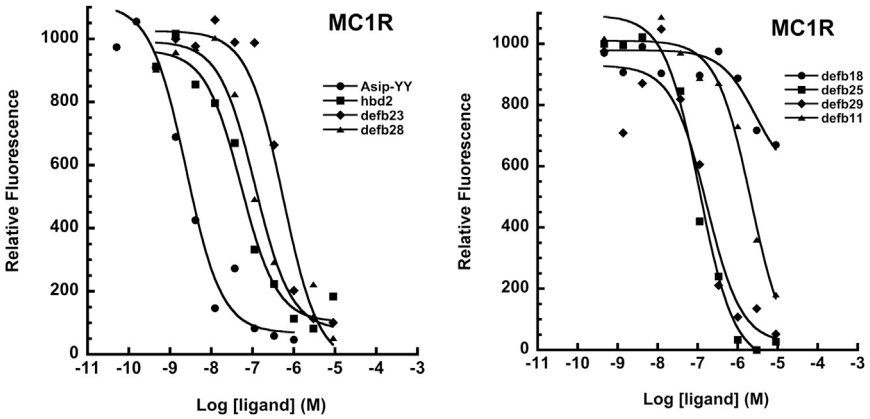

FIGURE 5 Competitive binding assays with Mc1r. A subset of competition binding assay curves in which varying amounts of unlabeled synthetic β-defensins were added together with Eu-NDP-MSH tracer to HEK293 cells transiently transfected with Mc1r. The logarithm of competing ligand concentration is plotted on the abscissa and the amount of Eu-NDP-MSH bound, measured as relative fluorescence, is plotted on the ordinate.

and 4 exhibited much weaker or no binding to Mc1r. Defb11 from cluster 3 displayed micromolar binding, whereas defb7, lacking a disulfide bond, did not exhibit any appreciable binding in our assay, which has an upper limit of measurable K_i of ~9 μM. With the exception of defb4 and defb18, we correctly predicted the Mc1r binding characteristics of seven (out of nine) selected members of the β-defensin family.

A visual comparison of the electrostatic surfaces of the select β-defensins fails to reveal any obvious features that distinguish high-affinity from low-affinity ligands (see Figs. S2 and 7). In an attempt to correlate the electrostatic properties of these peptides to their binding affinities, we plotted Mc1r K_i versus two metrics: net charge and Hodgkin ESI scores relative to HBD3 (Fig. 6). The correlation of net charge to K_i was insignificant, indicating that charge is a poor predictor of receptor binding ($R = 0.50$, $p = 0.145$). By contrast, the correlation between the Hodgkin ESI and K_i, while not strong, was moderately significant ($R = 0.66$, $p = 0.037$). Despite this correlation, one conspicuous discrepancy in the results strongly suggested inadequacies in either our analysis approach or the validity of our electrostatic binding model. Specifically, two peptides in our study, defb18 and defb25, had similar ESI scores but showed dramatically different behaviors at Mc1r. Both possess identical net charges and nearly identical ESI scores, yet defb18 exhibits no affinity for Mc1r, and defb25 exhibits a K_i of 27.8 nM for the receptor. We suspected that these two peptides may have been incorrectly assigned by our initial PIPSA analysis, and therefore sought to explore a more nuanced approach for the electrostatic and similarity calculations.

TABLE 1 Mc1r dissociation constants

Peptide	Cluster	Mc1r K_i (nM)[a]	Mean ± SE	Charge
ASIP-YY	NA	0.75	(0.13)	4
HBD3	1	33.0		11
defb4	1	3630.0		6
defb23	1	177.0	(25.4)	9
HBD2	1	22.9	(5.8)	6
defb28	2	35.2	(9.9)	8
defb18	2	NB		5
defb25	2	27.8	(7.8)	5
defb29	2	54.6	(15.1)	5
defb11	3	1581.4	(795.5)	1
defb7	4	NB		4

NB, no binding.

[a]All displacement binding experiments were performed using Eu-NDP-MSH as a competitor. Mean K_i values (in nM) were calculated by fitting the data to a sigmoidal dose-response curve with variable slope. The mean ± SE is reported in parentheses after each mean K_i value. All binding experiments were performed in triplicate or greater.

Our original similarity analysis compared members based on the entire surface area of the peptide structures, specifically the web-PIPSA default 4 Å skin around the entire solvent-accessible surface of each protein (16). (Although 4 Å is the commonly used default value, we note that a significantly different choice of skin thickness may alter the similarity ordering shown in Fig. 4.) However, it is most likely the case that compact ligands such as the β-defensins interact with Mc1r primarily through one specific region of their solvent-accessible surface. Therefore, our whole-surface analysis most likely weighs relevant and nonrelevant surfaces of the ligands equally, possibly skewing the overall similarity scoring result as it pertains to receptor binding. By restricting the similarity analysis solely to the relevant binding surface, we hoped to improve the correlation between the ESI score and the binding affinity. Unfortunately, the relevant binding surface of our benchmark β-defensin HBD3 is currently unknown and cannot be easily mapped by mutagenesis (13). However, this notion suggested that limiting our analysis to quadrants of the β-defensin structures might improve the electrostatic similarity scoring and its predictive power with regard to receptor binding, while simultaneously revealing the β-defensin binding surface that is most relevant for receptor affinity.

To guide more targeted regional calculations, we visually examined the electrostatic surfaces of defb18 and defb25 for differences that might account for their distinct binding affinities. Our inspection revealed that the largest difference

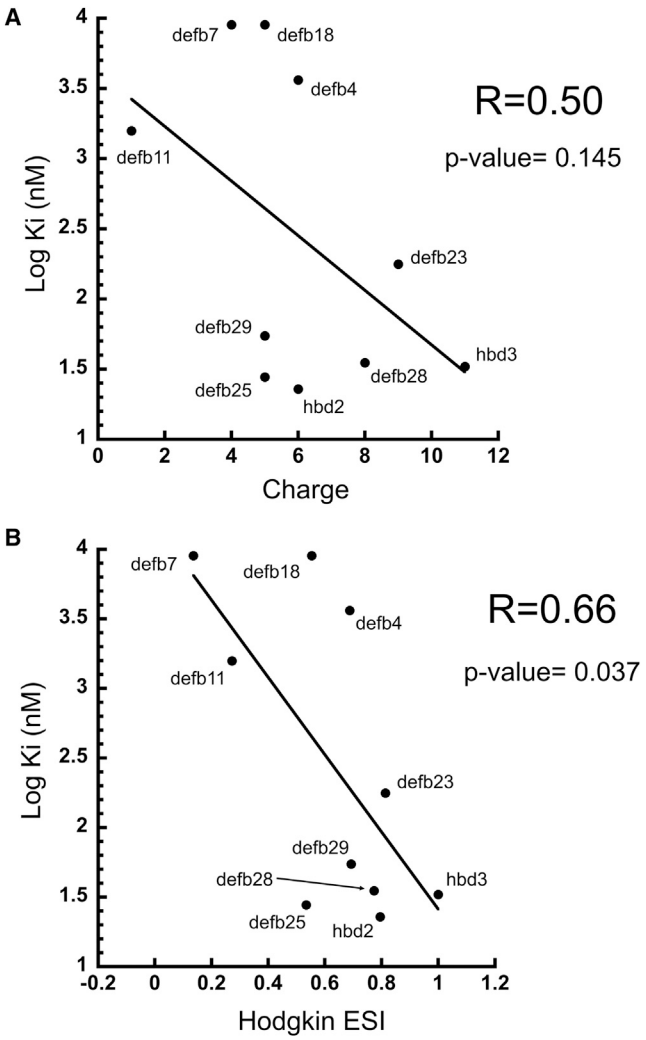

FIGURE 6 Correlation plots of peptide metrics versus binding affinity. (*A*) The net charge of the truncated version of each β-defensin tested is plotted on the abscissa and the log of K_i is plotted on the ordinate. (*B*) The Hodgkin ESI score for each β-defensin is plotted on the abscissa while the log of K_i is plotted on the ordinate. The Hodgkin ESI score is a single value ranging from -1 to 1, indicating how electrostatically similar each β-defensin is to HBD3. HBD3 compared with itself (completely similar) has an ESI of 1 (shown above on plot). Significance testing was performed using the program R.

between the two peptides was found in one particular region located on the north surface of the peptides as they are typically displayed. This region was approximately composed of two loops originating from segments found around and between Cys-2 and -3, and Cys-4 and -5, as well as a portion of the N-terminal α-helix (Fig. 7 *A*). We considered that variances in this region might account for the differences in binding affinity, and therefore performed additional calculations, restricting our analysis to this particular quadrant of the entire group of β-defensins. We performed our calculation using a sphere of 17 Å centered on a coordinate such that only the north electrostatic surface of each peptide was included in the similarity analysis (Fig. 7 *B*). Fig. 8 displays

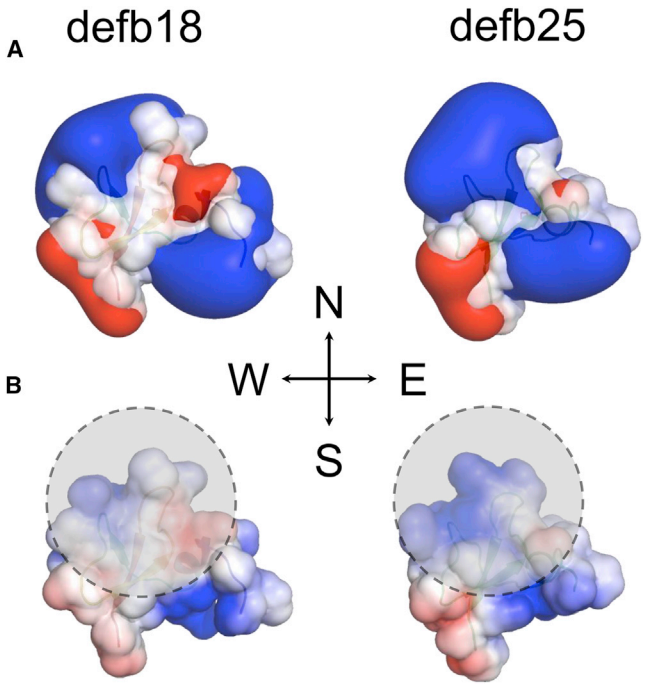

FIGURE 7 Electrostatic comparison of defb18 and defb25. (*A* and *B*) APBS-calculated electrostatic potentials of each peptide, shown with (*A*) a 1kT/e isocontour surface and (*B*) a solvent-accessible surface. Positive potential is shown in blue and negative potential is shown in red. The approximate shape and location of the 17 Å sphere where we performed our north-quadrant-targeted molecular-similarity analysis are shown as transparent dotted circles overlaid on the structures in (*B*).

the results of our 17 Å sphere calculation as raw Hodgkin ESI scores, and Fig. 9 displays the correlation plot of north ESI values versus Mc1r K_i affinity. We observed a slight resorting of the defb18 and defb25 peptides that more closely aligned with their observed binding (new ESI scores of 0.631 and 0.703, respectively), which contributed to a modest improvement of the ESI/Mc1r K_i correlation ($R = 0.71$, $p = 0.022$). By contrast, centering the same 17 Å sphere on the south region of the defensin structures demonstrated deterioration in the ESI/Mc1r correlation ($R = 0.49$, $p = 0.155$; data not shown). We also repeated this analysis on two additional sections of the defensin structure we termed the east and west quadrants (Fig. S3). Restricting the similarity analysis to the west quadrant displayed a poor correlation ($R = 0.56$, $p = 0.092$), whereas restricting the analysis to the east quadrant displayed a moderate correlation similar to the north-quadrant restriction ($R = 0.75$, $p = 0.012$).

DISCUSSION

All members of the melanocortin system were initially discovered through phenotype-driven approaches, and their genetic relationships with each other were established long before the structural biology behind their interactions was

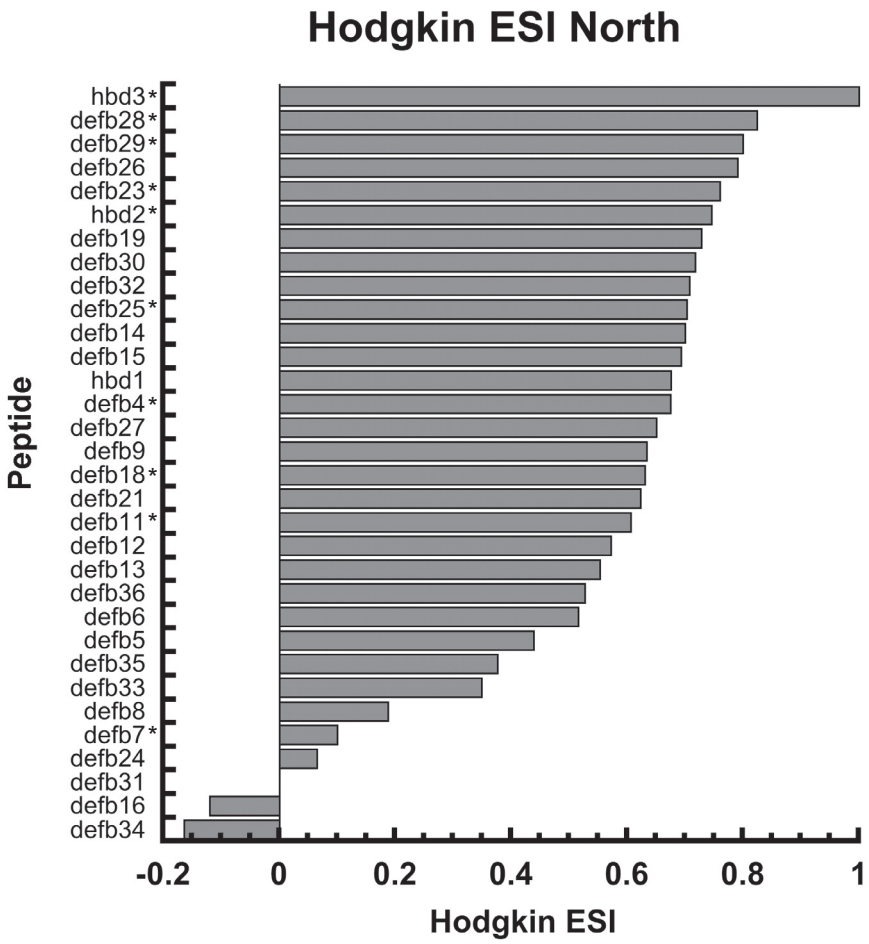

FIGURE 8 PIPSA Hodgkin ESIs for the north quadrant.

understood. Here, we present the results of an orthogonal approach that is capable of identifying new ligands of this receptor system based on molecular-similarity analysis. This protein-sequence and structure-driven strategy also provides a greater understanding of the molecular determinants of MCR binding. By ranking β-defensins based on their electrostatic similarity to HBD3, we correctly predicted the binding characteristics of seven out of nine select peptides. Moreover, through this analysis, we discovered five new (to our knowledge) Mc1r ligands with nanomolar affinity. In contrast, our search for a simple metric that drives a linear relationship between ESI and K_i was met with only limited success.

Our exploration of the β-defensin family identified several potential ligands for the melanocortin system, with implications for the biological function of this broad family of peptides. In humans, the β-defensins that we found to have high Mc1r affinity are expressed in a range of epithelial and other tissues, though several are exclusively found in the male reproductive tract (1,44). The distribution of these peptides, as well as their high affinity for Mc1r, suggests that they may serve a physiologically relevant signaling function in the melanocortin system. As Mc1r is known to operate in pigmentation as well as the immune system, our results expand the range of possible ligands that could modulate either of these phenotypes.

From this emerging perspective of the β-defensins and their dual capabilities as immune system molecules and ligands of Mc1r, our results might also explain certain melanistic phenotypes in coat-bearing animals. For instance, nearly 100% of the jaguars found on the Malaysian peninsula exhibit an all-black melanistic coat color, and one study has linked this anomaly to dominant mutations of Mc1r (45). However, it has been suggested that this coat color may be due to signaling pathways shared between the melanocortin and immune systems, and that melanistic coat color in some cases may be an artifact of past adaptions to pathogenic challenge (46). Our findings suggest that several members of the β-defensin family may account for the fixation of black coat color in these cats and possibly other animals with unexplained pigmentation effects. In this scenario, altered expression patterns of β-defensins that may have served as an adaptive response to microbial challenge could have also resulted in the pleiotropic coat-color effects observed today.

From a structural biology perspective, our findings also demonstrate that electrostatics alone can be a major determinant of MCR binding. Receptor-ligand interactions in

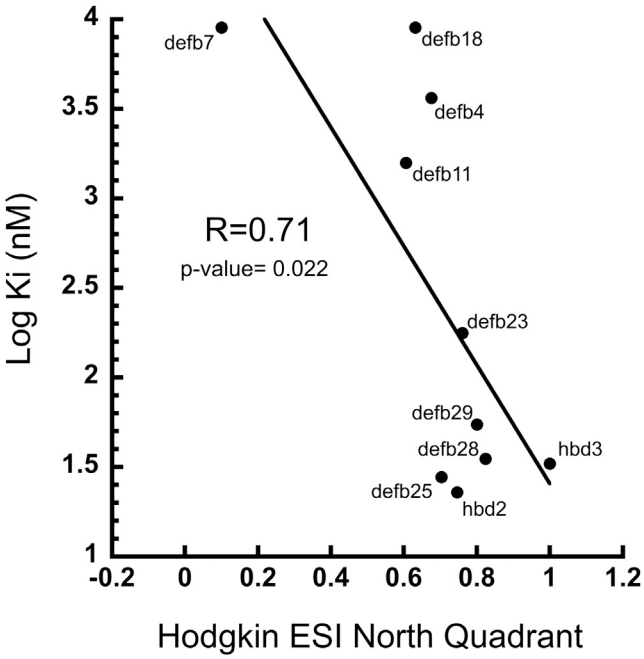

FIGURE 9 North-quadrant Hodgkin ESIs versus log K_i correlation plot.

the melanocortin system have typically been regarded as highly specific events, requiring the positive-aromatic pharmacophore that is present in most classic melanocortin ligands. At least in the case of these β-defensin peptides at Mc1r, a specific pharmacophore is not required, demonstrating the expansive promiscuity of this receptor. The peptides that bound Mc1r with high affinity share only two common features: disulfide bond topology and a specific arrangement of positively charged residues. Although the primary sequence of each defensin is different, according to our similarity analysis, the unique arrangement of charged residues in each one generates a similar positive electrostatic potential field. Although our electrostatic analysis strongly implies that their Mc1r binding capabilities are due to this common physicochemical feature, the modest correlation between the Hodgkin ESIs and K_i suggests that other important β-defensin features are missing from our analysis. In contrast to our electrostatic model of binding, a previous structural investigation of heterodimer protein complexes showed that charged residues such as Arg and Lys are typically less abundant in the interface region, whereas aliphatic and aromatic residues are enriched (47). Although the MCRs may represent a unique case of protein-protein interaction facilitated mostly by charged residues at the interface, it may be that other residues that are not captured by electrostatic analysis contribute to receptor binding affinity.

It is certainly possible that our analysis can be improved purely through computational means. As is the case in most protein-protein interactions, the β-defensins most likely interface with the receptor using a specific peptide surface region that is more critical for receptor affinity.

Our initial method of comparing electrostatic potentials took into account the entire protein surface, which may not be an ideal approach. Our targeted similarity analysis, focusing roughly on four quadrants of the defensin structure, demonstrated significant improvements in the correlation between ESI and Mc1r K_i when we restricted the similarity analysis to the north and east quadrants. Although these results are speculative, they suggest a general orientation of the defensins relative to the receptors and that the relevant surface necessary for their interaction lies somewhere within this half of the protein. Further structural studies will be required to confirm our proposed binding orientation of these ligands at Mc1r.

These results may also provide insight into the binding determinants of β-defensins in other receptor systems. In this study, we found that HBD2 bound tightly to Mc1r with an affinity similar to that of HBD3. Both HBD2 and HBD3 have demonstrated anti-HIV properties, inhibiting infection through direct interaction with the virus and preventing its entry into cells by interaction with the chemokine receptor CXCR4 (48,49). The structure of CXCR4 was recently published, and interestingly shows a ligand-binding domain that is highly negative, similar to the MCRs (50). The ligands and electrostatic features shared by CXCR4 and the MCRs suggest to us that a similar electrostatic interaction may operate between the β-defensins and both receptor classes. Further work will be required to determine the exact binding mechanism of either β-defensin at CXCR4.

Our electrostatic analysis of β-defensins also demonstrates the utility of in silico methods for discriminating binding affinity in cases involving excessive and oppositely charged molecules. Our analysis of the β-defensin family covered only a small percentage of potential peptide ligands available for consideration in the UniProt database. We envision that, due to the loose requirements of MCR binding we observed, several more ligands for these receptors may exist and provide functionality in this system. By applying electrostatic similarity analysis to a wider range of molecules, investigators may be able to identify these ligands, although improved methods for efficiently performing such a large-scale analysis would be required.

Finally, the importance of electrostatics demonstrated here also suggests that this feature could be used in the design of new compounds for binding and activity in the melanocortin system. Several groups have proposed the electrostatic design or optimization of proteins when excessive electrostatic complementarity is important for system function (51-53). Several of these β-defensins bind to other GPCRs, and electrostatics may similarly play a part in their function. As such, this approach might also be extended to other GPCR systems in which electrostatic binding forces are dominant.

SUPPORTING MATERIAL

Three figures are available at http://www.biophysj.org/biophysj/supplemental/S0006-3495(15)00937-6.

AUTHOR CONTRIBUTIONS

M.A.N., C.B.K., G.S.B., and G.L.M. designed the research. M.A.N., C.B.K., R.P., and J.M. performed the experiments. M.A.N., C.B.K., G.S.B., and G.L.M. analyzed the data. M.A.N. and G.L.M. wrote the manuscript, with input and edits from all of the authors.

ACKNOWLEDGMENTS

This work was supported by National Institutes of Health grant DK064265 (to G.L.M.).

REFERENCES

1. Pazgier, M., D. M. Hoover, …, J. Lubkowski. 2006. Human beta-defensins. *Cell. Mol. Life Sci.* 63:1294–1313.
2. Candille, S. I., C. B. Kaelin, …, G. S. Barsh. 2007. A -defensin mutation causes black coat color in domestic dogs. *Science.* 318:1418–1423.
3. Yang, D., O. Chertov, …, J. J. Oppenheim. 1999. Beta-defensins: linking innate and adaptive immunity through dendritic and T cell CCR6. *Science.* 286:525–528.
4. Gantz, I., and T. M. Fong. 2003. The melanocortin system. *Am. J. Physiol. Endocrinol. Metab.* 284:E468–E474.
5. Ghamari-Langroudi, M., G. J. Digby, …, R. D. Cone. 2015. G-protein-independent coupling of MC4R to Kir7.1 in hypothalamic neurons. *Nature.* 520:94–98.
6. Barsh, G. S. 2006. Regulation of pigment type-switching by agouti, melanocortin signaling, attractin, and mahoganoid. *In* The Pigmentary System. J. J. Nordlund, R. E. Boissy, V. J. Hearing, R. A. King, W. S. Oetting, and J. Ortonne, editors. Blackwell, Oxford.
7. Robbins, L. S., J. H. Nadeau, …, R. D. Cone. 1993. Pigmentation phenotypes of variant extension locus alleles result from point mutations that alter MSH receptor function. *Cell.* 72:827–834.
8. Klungland, H., and D. I. Vage. 2003. Pigmentary switches in domestic animal species. *Ann. N. Y. Acad. Sci.* 994:331–338.
9. Yang, Yk., C. Dickinson, …, I. Gantz. 1997. Molecular basis for the interaction of [Nle4,D-Phe7]melanocyte stimulating hormone with the human melanocortin-1 receptor. *J. Biol. Chem.* 272:23000–23010.
10. Kiefer, L. L., J. M. Veal, …, W. O. Wilkison. 1998. Melanocortin receptor binding determinants in the agouti protein. *Biochemistry.* 37:991–997.
11. Tota, M. R., T. S. Smith, …, T. M. Fong. 1999. Molecular interaction of Agouti protein and Agouti-related protein with human melanocortin receptors. *Biochemistry.* 38:897–904.
12. Yang, Y. K., D. A. Thompson, …, I. Gantz. 1999. Characterization of Agouti-related protein binding to melanocortin receptors. *Mol. Endocrinol.* 13:148–155.
13. Nix, M. A., C. B. Kaelin, …, G. L. Millhauser. 2013. Molecular and functional analysis of human β-defensin 3 action at melanocortin receptors. *Chem. Biol.* 20:784–795.
14. Maldonado, A. G., J. P. Doucet, …, B. T. Fan. 2006. Molecular similarity and diversity in chemoinformatics: from theory to applications. *Mol. Divers.* 10:39–79.
15. Wade, R. C., R. R. Gabdoulline, and F. De Rienzo. 2001. Protein interaction property similarity analysis. *Int. J. Quantum Chem.* 83:122–127.
16. Richter, S., A. Wenzel, …, R. C. Wade. 2008. webPIPSA: a web server for the comparison of protein interaction properties. *Nucleic Acids Res.* 36:W276–W280.
17. Sali, A., and T. L. Blundell. 1993. Comparative protein modelling by satisfaction of spatial restraints. *J. Mol. Biol.* 234:779–815.
18. UniProt Consortium. 2015. UniProt: a hub for protein information. *Nucleic Acids Res.* 43:D204–D212.
19. Pettersen, E. F., T. D. Goddard, …, T. E. Ferrin. 2004. UCSF Chimera—a visualization system for exploratory research and analysis. *J. Comput. Chem.* 25:1605–1612.
20. Baker, N. A., D. Sept, …, J. A. McCammon. 2001. Electrostatics of nanosystems: application to microtubules and the ribosome. *Proc. Natl. Acad. Sci. USA.* 98:10037–10041.
21. Dolinsky, T. J., P. Czodrowski, …, N. A. Baker. 2007. PDB2PQR: expanding and upgrading automated preparation of biomolecular structures for molecular simulations. *Nucleic Acids Res.* 35:W522–W525.
22. Hodgkin, E. E., and S. Richter. 1987. Molecular similarity based on electrostatic potential and electric field. *Int. J. Quant. Chem.* 32::105–110.
23. R Core Team. 2009. R: A Language and Environment for Statistical Computing. R Foundation for Statistical Computing, Vienna, Austria.
24. Schulz, A., E. Klüver, …, K. Adermann. 2005. Engineering disulfide bonds of the novel human beta-defensins hBD-27 and hBD-28: differences in disulfide formation and biological activity among human beta-defensins. *Biopolymers.* 80:34–49.
25. Kamber, B., A. Hartmann, …, W. Rittel. 1980. The synthesis of cystine peptides by iodine oxidation of S-trityl-cysteine and S-acetamidomethyl-cysteine peptides. *Helv. Chim. Acta.* 63:899–915.
26. Akaji, K., T. Tatsumi, …, Y. Kiso. 1992. Disulfide bond formation using the silyl chloride sulfoxide system for the synthesis of a cystine peptide. *J. Am. Chem. Soc.* 114:4137–4143.
27. Schibli, D. J., H. N. Hunter, …, H. J. Vogel. 2002. The solution structures of the human beta-defensins lead to a better understanding of the potent bactericidal activity of HBD3 against Staphylococcus aureus. *J. Biol. Chem.* 277:8279–8289.
28. Hoover, D. M., K. R. Rajashankar, …, J. Lubkowski. 2000. The structure of human beta-defensin-2 shows evidence of higher order oligomerization. *J. Biol. Chem.* 275:32911–32918.
29. Hoover, D. M., O. Chertov, and J. Lubkowski. 2001. The structure of human beta-defensin-1: new insights into structural properties of beta-defensins. *J. Biol. Chem.* 276:39021–39026.
30. De Paula, V. S., N. S. Gomes, …, A. P. Valente. 2013. Structural basis for the interaction of human β-defensin 6 and its putative chemokine receptor CCR2 and breast cancer microvesicles. *J. Mol. Biol.* 425:4479–4495.
31. Bauer, F., K. Schweimer, …, H. Sticht. 2001. Structure determination of human and murine beta-defensins reveals structural conservation in the absence of significant sequence similarity. *Protein Sci.* 10:2470–2479.
32. Schutte, B. C., J. P. Mitros, …, P. B. McCray, Jr. 2002. Discovery of five conserved beta-defensin gene clusters using a computational search strategy. *Proc. Natl. Acad. Sci. USA.* 99:2129–2133.
33. Rouvray, D. H. 1990. The evolution of the concept of molecular similarity. *In* Concepts and Applications of Molecular Similarity. M. A. Johnson and G. M. Maggiora, editors. John Wiley & Sons, New York.
34. Todeschini, A. R., and V. Consonni. 2000. Handbook of Molecular Descriptors. Wiley-VCH, Weinheim, Germany.
35. Nikolova, N., and J. Jaworska. 2003. Approaches to measure chemical similarity—a review. *QSAR Comb. Sci.* 22:1006–1026.
36. Lipinski, C. A., F. Lombardo, …, P. J. Feeney. 2001. Experimental and computational approaches to estimate solubility and permeability in drug discovery and development settings. *Adv. Drug Deliv. Rev.* 46:3–26.
37. Holliday, J. D., C. Y. Hu, and P. Willett. 2002. Grouping of coefficients for the calculation of inter-molecular similarity and dissimilarity

using 2D fragment bit-strings. *Comb. Chem. High Throughput Screen.* 5:155–166.

38. Adamson, G. W., and J. A. Bush. 1975. A comparison of the performance of some similarity and dissimilarity measures in the automatic classification of chemical structures. *J. Chem. Inf. Comput. Sci.* 15:55–58.
39. Fogolari, F., A. Brigo, and H. Molinari. 2002. The Poisson-Boltzmann equation for biomolecular electrostatics: a tool for structural biology. *J. Mol. Recognit.* 15:377–392.
40. Gouy, M. 1910. Sur la constitution de la charge électrique à la surface d'un électrolyte. *J. Phys. Théor. Appl.* 9:457–468.
41. Chapman, D. L. 1913. A contribution to the theory of electrocapillarity. *Philos. Mag.* 25:475–481.
42. Debye, P., and E. Huckel. 1923. Zur Theorie der Elektrolyte. *Phys. Z.* 24:185–206.
43. McNulty, J. C., P. J. Jackson, …, G. L. Millhauser. 2005. Structures of the agouti signaling protein. *J. Mol. Biol.* 346:1059–1070.
44. Harder, J., J. Bartels, …, J. M. Schröder. 1997. A peptide antibiotic from human skin. *Nature.* 387:861.
45. Eizirik, E., N. Yuhki, …, S. J. O'Brien. 2003. Molecular genetics and evolution of melanism in the cat family. *Curr. Biol.* 13:448–453.
46. Sunquist, F. 2006. Malaysian mystery leopards. *In* National Wildlife. National Wildlife Federation, Reston, VA.
47. Bahadur, R. P., and M. Zacharias. 2008. The interface of protein-protein complexes: analysis of contacts and prediction of interactions. *Cell. Mol. Life Sci.* 65:1059–1072.
48. Quiñones-Mateu, M. E., M. M. Lederman, …, A. Weinberg. 2003. Human epithelial beta-defensins 2 and 3 inhibit HIV-1 replication. *AIDS.* 17:F39–F48.
49. Weinberg, A., M. E. Quiñones-Mateu, and M. M. Lederman. 2006. Role of human beta-defensins in HIV infection. *Adv. Dent. Res.* 19:42–48.
50. Wu, B., E. Y. Chien, …, R. C. Stevens. 2010. Structures of the CXCR4 chemokine GPCR with small-molecule and cyclic peptide antagonists. *Science.* 330:1066–1071.
51. Gorham, R. D., Jr., C. A. Kieslich, and D. Morikis. 2011. Electrostatic clustering and free energy calculations provide a foundation for protein design and optimization. *Ann. Biomed. Eng.* 39:1252–1263.
52. Henrich, S., S. Richter, and R. C. Wade. 2008. On the use of PIPSA to guide target-selective drug design. *ChemMedChem.* 3:413–417.
53. Vizcarra, C. L., and S. L. Mayo. 2005. Electrostatics in computational protein design. *Curr. Opin. Chem. Biol.* 9:622–626.